



# Lightning Current Distribution in the Components of Cladding Structure

Oleksii Bondar

Institute of Electrodynamics, NASU  
Kyiv, Ukraine  
[bondar\\_o\\_i@ukr.net](mailto:bondar_o_i@ukr.net)

Volodymyr Shostak

NTUU "Kyiv Polytechnic Institute"  
Kyiv, Ukraine  
[Volod\\_Shostak@ukr.net](mailto:Volod_Shostak@ukr.net)

Thomas Smatloch

Dehn + Söhne GmbH + Co.KG.  
Neumarkt, Germany  
[thomas.smatloch@dehn.de](mailto:thomas.smatloch@dehn.de)

**Abstract** — Results on numerical simulation (NS) of lightning current distribution in components of round standing seam cladding structure are presented. NS was performed by using 3D models of two types: large-scale model (#1), better reproducing conditions for current distribution in natural cladding; small model (#2), reproducing the sample for laboratory tests. Analysis included cases related to injection of lightning current having different standard waveforms (approximations) and variation of some parameters (halter's fastening contact area, channel radius and length). Scaling effects on using small test samples are addressed and recommendations for selection of adequate current parameters during tests are provided. In particular, in approach of equivalent frequency, for impulse waveform 10/350  $\mu$ s and basic dimensions of the cladding components, current magnitude portion distributed into main halter (under the strike point) for the small model #2 (13.5 %) is obtained about twice bigger than that for the large one #1 (7 %). For continuous current, corresponding current portions are almost identical for both models: #1 – 45%, #2 – 43.5%. More accurate proportions of possible magnitude correction can be determined in further studies by considering closer waveform approximation and tests.

**Keywords** - finite element method; lightning current distribution; lightning protection system; roof cladding structure; lightning tests

## I. INTRODUCTION

Metallic roof or wall cladding is usually made of thin sheets having thickness typically within 0.5 to 1.2 mm from various materials (copper, aluminum, galvanized steel, stainless steel and other). In most cases of direct lightning strikes to the structure without lightning protection (LP), such thin cladding will be melted and perforated by continuous or impulse current components. Characteristic dimensions of observed holes are from a few millimeters to centimeters, but can be larger [1-3].

When such damage is not accepted for considered structures, some LP solution is required. When due to some reasons (budget, services, technical, risk assessment and other issues) such damage can be accepted, the external parts of the cladding can be used as natural component for lightning

termination and for conducting its current down to ground, but certain conditions to be satisfied according LP standards [4]. One of these is the minimal thickness of metal sheets. In case of steel it is 0.5 mm, when it is not important to prevent puncture, hot spot or ignition problem. Another one condition to be mentioned here is that in cladding (and roof) structure it is provided electrical continuity between various parts. Note, that these requirements are considered as factors related to all classes of lightning protection systems (LPS).

For large structures, like airport terminals, hangars, etc., a so-called standing seam cladding systems is widely used (for example, see [5] or model sketches in Fig. 1 of present work). For these, typical sheet thickness is 0.8 to 1.2 mm. The sheets having seams are placed and sliding on supporting metal clips (halters, Fig. 1b), which are fastened to the metallic base roof structure by some screws. When one accepts the use of such cladding without external LP, he must also check the operation conditions for other layers located below the metal sheets (water proof and other barriers, sealing membranes, insulation). In relation to lightning effects upon cladding, these conditions depend on the possibility of melted metal to cause some damage to mentioned layers, on the electrodynamic forces (EDF) at the cladding structure during action of lightning having extreme current parameters, on the temperature regime and EDF at the fastening elements (e.g., halter's screws).

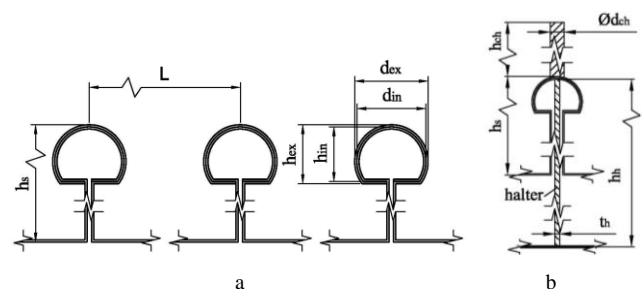


Figure 1. Cross-section views of the cladding model: a – seams; b - details on elements "channel - cladding seam - halter"

The complexity of the described system and processes requires analysis of mentioned factors and performing of some tests at cladding samples by standard lightning currents according to accepted LP level for the structure [6]. Analysis may include simulation of current distribution at components of the cladding structure, thermal studies, etc. Preliminary estimations on current distribution for such type of cladding having round standing seams were started by authors using simplified 2D-approach in [7], and a more detailed numerical simulation (NS) was continued by using 3D-approach in [8]. In these studies, we considered rather small thickness of the sheet (0.6 mm), and as material of the cladding components the stainless steel was accepted (these satisfy the requirements of [4],  $\geq 0.5$  mm). To the best of our knowledge, for the time no other works have addressed this issue for such cladding type.

Regarding tests, it is important to estimate the influence of scaling factors when one using cladding test samples of reduced dimensions. Usually limitations to these samples are determined by test stand geometry, as it should be compact to simultaneously provide required current waveform magnitude and steepness.

The aim of present study is to develop more sophisticated 3D models for cladding and provide simulations of current distribution among its components, namely in metal sheet and clips in vicinity of lightning strike point. The worse case of lightning striking the seam just above the halter is considered here. Also, the analysis is including comparison of mentioned distributions for two models: large (#1), reproducing larger piece of natural cladding, and small (#2), reproducing sample for the laboratory test stand. Influence of variation dimensions of some cladding components (halter fastening contact area) and channel (radius, length), and test current parameters (various waveforms) are addressed too. Then recommendations are provided regarding accounting of scaling effects when current parameters to be selected for the tests.

## II. MODELS GEOMETRY

As mentioned, two main models are considered. In both models cross-section views and dimensions of seams and

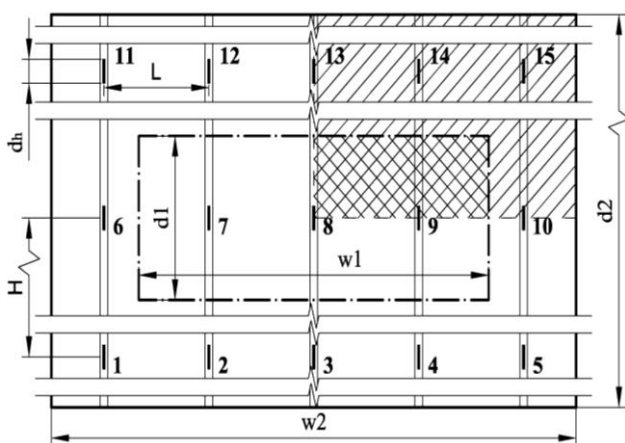


Figure 2. Models' dimensions and relation (large & small, full & ¼)

halters are identical (see Fig. 1). Full two models have following top-view dimensions: #1 –  $d_2 \times w_2 = 2850 \times 1500$  mm and #2 –  $d_1 \times w_1 = 400 \times 1000$  mm (Fig. 2). Model #2 is shown as small portion of the larger model #2. In Fig. 2, positions 1 to 8 are indicating the locations of halters. “Main” halter, that receives the major current portion, is at position 8. The step of halters is  $H = 0.85$  m and step of seams is  $L = 0.3$  m. Seam's height is  $h_s = 65$  mm. In Fig. 1:  $d_{in} = 20$  mm,  $d_{ex} = 21.2$  mm,  $h_{in} = 15$  mm,  $h_{ex} = 16.2$  mm. Halter's width is  $d_h = 58$  mm (along seam, Fig. 2), height  $h_h$  is about 128 mm, and thickness of the “leg” is  $t_h = 2$  mm (Fig. 1b). Contact area at the halter's fastening zone is assumed  $2 \times 58$  mm<sup>2</sup> and, in other variant,  $1 \times 58$  mm<sup>2</sup>. For most calculations, lightning channel diameter was assumed  $d_{ch} = 6$  mm, and for selected variants ( $f = 0$  and 25 kHz) it was taken  $d_{ch} = 15$  mm; channel height –  $h_{ch} = 47$  mm. The numbers on channel radius are based on results of observations, tests and analysis described in [2, 3, 10].

Two cross-hatched areas are indicating ¼ portions (quarter sections) of the two full models. These reduced models were used in most calculations by applying special conditions of symmetry. Full models were utilized only in some cases to double check the correctness of reduced models. The 3D-views of these full and ¼ models are shown in Figs. 3 and 4.

## III. COMPUTATIONAL METHOD AND MODELING CONDITIONS

### A. Computational Method

Computations of lightning current distribution in LPS can be carried out using different approaches, which in general are based on electrical circuit theory and electromagnetic field theory. When lightning current is injected into objects of complex geometry, it is appropriate to apply numerical methods based on electromagnetic field theory (finite element method (FEM), finite difference time domain method (FDTD), method of moments (MoM) or other). This paper presents results obtained by numerical electromagnetic analysis using finite element method (FEM) in frequency domain.

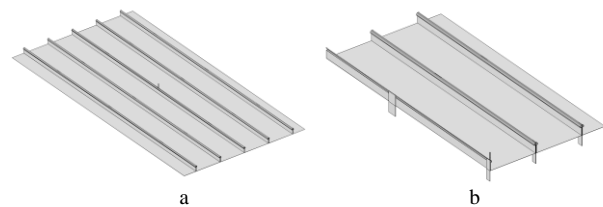


Figure 3. Full (a) and reduced to ¼ (b) large models, #1

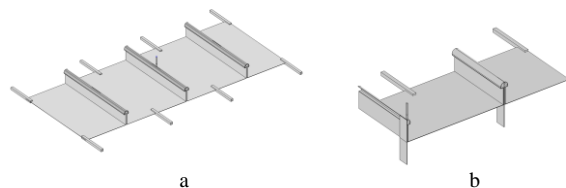


Figure 4. Full (a) and reduced to ¼ (b) small models, #2

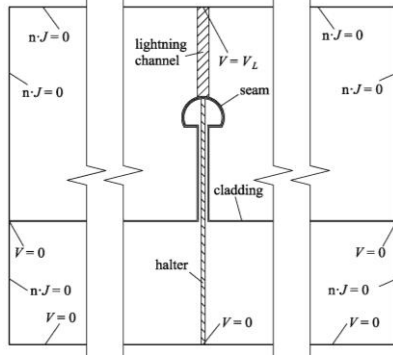


Figure 5. Example of computational domain cross-section: lightning channel, cladding having standing seam, and halter surrounded by air

Simulations are performed using predefined physics in the Comsol Multiphysics software: “Magnetic and electric fields (mef)” – for modeling first positive, first negative, subsequent lightning strokes, and continuous current [6]; and “Electric currents (ec)” – for modeling continuous current.

#### B. Calculation Model and Boundary Conditions

Calculation model consists of following subdomains (Fig. 5): cladding, halters, lightning channel, earthed base structure and air. Electric potential  $V_L$  has been applied at the top of the lightning channel to provide needed current. Bottoms of the halters, external edges of the cladding, and bottom of the computational domain were grounded. At some external boundaries, electric insulation boundary condition ( $\mathbf{n} \cdot \mathbf{J} = 0$ ) has been applied; and on all external boundaries, magnetic insulation boundary condition ( $\mathbf{n} \cdot \mathbf{A} = 0$ ) was applied too. In some cases, when only  $\frac{1}{4}$  of the model is considered, a perfect magnetic conductor boundary condition ( $\mathbf{n} \times \mathbf{H} = 0$ ,  $\mathbf{n} \cdot \mathbf{J} = 0$ ) has been applied at the boundaries of symmetry.

#### C. Current Waveforms

In frequency domain, standard impulse components of lightning current [6] are simulated by an oscillating waveform exhibiting some equivalent frequency related to impulse front time: 25 kHz – for the first positive lightning stroke, 250 kHz – for the first negative lightning stroke, 1 MHz – for the subsequent lightning stroke [9]. Continuous current is simulated also by an oscillating waveform having frequency of 1 Hz. For full models it was simulated also as constant current ( $f = 0$  Hz).

#### D. Material Characteristics

Only two mediums and related electrical characteristics for modeling subdomains are considered in this paper (Table I): air (for air subdomain) and stainless steel (for halters, cladding sheet, and channel subdomains).

TABLE I. ELECTRICAL CHARACTERISTICS OF THE MODELING SUBDOMAINS

Medium	$\epsilon_r$	$\mu_r$	$\sigma, \Omega/m$	
1	air	1	1	0
2	stainless steel	1	1	$1.429 \cdot 10^6$

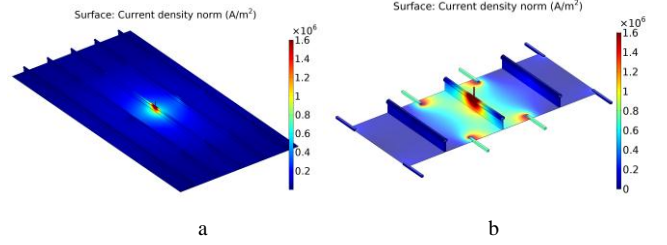


Figure 6. Current density distribution in two full models of the cladding: a) #1 (large) and b) #2 (test sample);  $f = 0$  Hz

## IV. SIMULATION RESULTS

### A. Full Models #1 and #2

Results on current density distributions at the surfaces of cladding for the two full models are shown in Fig. 6. These are related to  $f = 0$  Hz. Note, that in these and all following diagrams, top limit number at the scale ruler on the right hand shows that the top color corresponds in diagram to zones, in which current densities are not lower than this level. Also, following parameters are used in simulations presented in all current density diagrams:  $t_h = 2$  mm and  $d_{ch} = 6$  mm. Results related to some other values of these parameters are included further in corresponding Tables.

Results on current distributions between halters for the discussed two full models and  $f = 0$  Hz are gathered in Tables II and III. In latest, data also presented for other values of parameters ( $t_h = 1$  mm and  $d_{ch} = 15$  mm). Data indicate the absence of  $t_h$  and  $d_{ch}$  noticeable influence upon current distribution for considered case associated with continuous current. Parameter  $t_h = 1$  mm is related to smaller contact area ( $1 \times 58$  mm<sup>2</sup>) at the fastening zone of the halter, which is accounted in simulation by transition to 1mm at the halter’s last 5-mm bottom section, from its regular width ( $t_h = 2$  mm).

TABLE II. CURRENT DISTRIBUTION BETWEEN HALTERS FOR FULL MODEL #1 (LARGE),  $f = 0$  HZ

Current portions in halters, %							
18	19	110	111	112	113	114	115
44.97	5.90	1.33	0.55	1.72	2.43	1.72	0.55

TABLE III. CURRENT DISTRIBUTION BETWEEN HALTERS FOR FULL MODEL #2 (SMALL),  $f = 0$  HZ

Parameters		Current portions in halters, %		
$d_{ch}, mm$	$t_h, mm$	17	18	19
6	2	2.76	43.49	2.76
	1	2.75	42.52	2.74
15	2	2.78	42.97	2.78

### B. Reduced Models #1 and #2 (Quarter Sections)

Results on current density distributions for the two reduced models (quarter sections) are shown in Figs. 7 and 8. These are related to  $f = 1$  Hz, 25 kHz, 250 kHz, and 1 MHz. Calculated portions of current distributions for these cases are collected in Tables IV and V. Again, for the model #2 (small), some results are presented also for other values of parameters ( $t_h = 1$  mm and  $d_{ch} = 15$  mm), which indicate no their visible

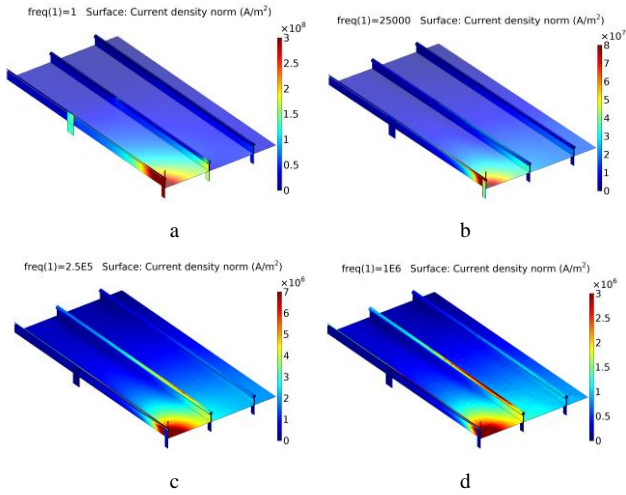


Figure 7. Current density distribution in reduced model #1 (large): a)  $f = 1$  Hz, b)  $f = 25$  kHz, c)  $f = 250$  kHz, d)  $f = 1$  MHz

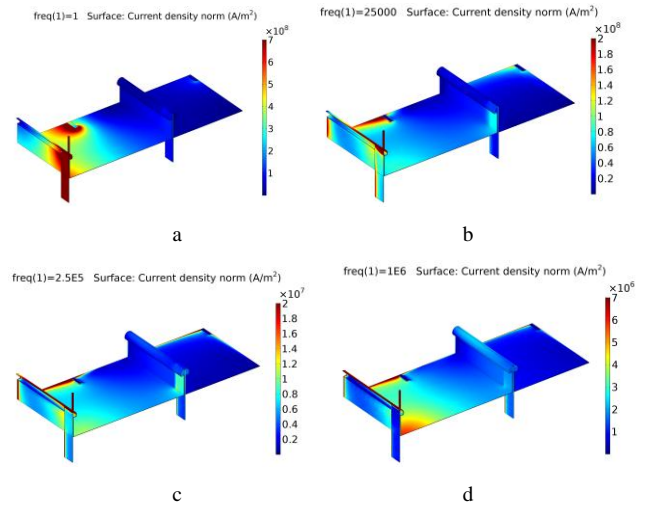


Figure 8. Current density distribution in reduced model #2 (test sample): a)  $f = 1$  Hz, b)  $f = 25$  kHz, c)  $f = 250$  kHz, d)  $f = 1$  MHz

TABLE IV. CURRENT DISTRIBUTION BETWEEN HALTERS FOR REDUCED MODEL #1 (LARGE,  $\frac{1}{4}$  SECTION)

$f$ , kHz	Current portions in halters, %					
	I18	I19	I10	I13	I14	I15
0.001	45.02	5.92	1.34	2.44	1.73	0.55
25	7.01	0.24	0.04	0.38	0.26	0.08
250	0.71	0.02	0.01	0.02	0.01	0.00
1000	0.16	0.01	0.00	0.00	0.00	0.00

TABLE V. CURRENT DISTRIBUTION BETWEEN HALTERS FOR REDUCED MODEL #2 (SMALL,  $\frac{1}{4}$  SECTION)

Parameters			Current portions in halters, %	
$d_{ch}$ , mm	$t_b$ , mm	$f$ , kHz	I18	I19
6	2	0.001	43.49	2.76
		25	13.46	8.85
		250	11.32	9.16
		1000	9.21	6.64
15	1	25	13.45	8.83
	2	25	13.45	8.87

influence upon current distribution between halters for considered equivalent frequency 25 kHz.

For reduced models were performed also preliminary simulations for different channel lengths up to  $h_{ch} = 0.2$  m, which show variation of current portion to main halter within about 10%.

## V. CONCLUSION

Several peculiarities and differences are observed for continuous and impulse currents, small and large models. In general, during application of impulses (equivalent frequency approximation,  $f = 25, 250, 1000$  kHz), at least up to peak current, much lower its portion is going into the “main” halter located under the point of strike in case of large model. Thus, during impulse tests, it looks that small test samples present somewhat more severe conditions for the main halter and its screws, than in case of large cladding. This indicates to the

need of possible impulse current magnitude correction (reduction) in tests of small samples to better reproduce conditions for the large cladding area. Exact proportions of magnitude correction can be studied in further research. For continuous current, such reduction is not significant.

## ACKNOWLEDGMENT

O. B. deeply appreciates helpful advices of colleague Oleksandr Hlukhenkyi on the application of special software to numerical simulation of considered problems.

## REFERENCES

- [1] H. E. Sueta, N.V.B. Alves, J. A. B. Grimoni, G. F. Burani, “Lightning current charge estimation by the analysis on the damages in metallic roofs,” Intl. Conf. on Grounding and Earthing & 2nd Intl Conf. on Lightning Physics and Effects, Maceió, Brazil, pp.1-5, 2006.
- [2] M.I. Baranov, V.I. Kravchenko, M.A. Nosenko, “Experimental researches of electro-thermal stability of metallic elements of aircraft to direct action of current of artificial lightning. Part 1: Stability of the aluminum edging,” Elektrotehnika s Elektromekhanika, No. 1, pp.65-71, 2011.
- [3] Lightning Protection/Earthing, – <https://www.dehn-international.com/en>.
- [4] IEC 62305-3: 2010. Protection Against Lightning – Part III: Physical damage to structures and life hazard.
- [5] Kalzip systems – Product information, application and specification, 2011.
- [6] IEC 62305-1: 2010. Protection Against Lightning – Part 1: General principles.
- [7] V. O. Shostak, O. I. Bondar, “Simulation of lightning current distributions at elements of lightning protection system”, Conf. on Modern problems in Power Elctrotechnique and Automation, NTUU «KPI», Kyiv: «Polytechnika», pp. 457-458, 2012.
- [8] O. I. Bondar, V. O. Shostak, “Metallic thin cladding in lightning protection system: current distribution between clips”, Conf. on Modern problems in Power Elctrotechnique and Automation, NTUU «KPI», Kyiv: «Polytechnika», pp. 361-363, 2015.
- [9] S. F. Madsen, C. F. Mieritz, “Current distribution and magnetic fields in complex structures using Comsol Multiphysics”, Proc. Comsol Conf., Stuttgart, pp.1-7, 2011.
- [10] M. A. Uman, Lightning, New York: McGraw-Hill Book Company, 1969.